Single rat muscle Na^+ channel mutation confers batrachotoxin autoresistance found in poison-dart frog *Phyllobates terribilis*

Sho-Ya Wang[a,1] and Ging Kuo Wang[a]

[a]Department of Biological Sciences, State University of New York at Albany, Albany, NY 12222

Edited by Richard W. Aldrich, The University of Texas at Austin, Austin, TX, and approved August 8, 2017 (received for review May 12, 2017)

Poison-dart *Phyllobates terribilis* frogs sequester lethal amounts of steroidal alkaloid batrachotoxin (BTX) in their skin as a defense mechanism against predators. BTX targets voltage-gated Na^+ channels and enables them to open persistently. How BTX autoresistance arises in such frogs remains a mystery. The BTX receptor has been delineated along the Na^+ channel inner cavity, which is formed jointly by four S6 transmembrane segments from domains D1 to D4. Within the *P. terribilis* muscle Na^+ channel, five amino acid (AA) substitutions have been identified at D1/S6 and D4/S6. We therefore investigated the role of these naturally occurring substitutions in BTX autoresistance by introducing them into rat Nav1.4 muscle Na^+ channel, both individually and in combination. Our results showed that combination mutants containing an N1584T substitution all conferred a complete BTX-resistant phenotype when expressed in mammalian HEK293t cells. The single N1584T mutant also retained its functional integrity and became exceptionally resistant to 5 μM BTX, aside from a small residual BTX effect. Single and combination mutants with the other four S6 residues (S429A, I433V, A445D, and V1583I) all remained highly BTX sensitive. These findings, along with diverse BTX phenotypes of N1584K/A/D/T mutant channels, led us to conclude that the conserved N1584 residue is indispensable for BTX actions, probably functioning as an integral part of the BTX receptor. Thus, complete BTX autoresistance found in *P. terribilis* muscle Na^+ channels could emerge primarily from a single AA substitution (asparagine→threonine) via a single nucleotide mutation (AAC→ACC).

poison-dart frogs | batrachotoxin | autoresistance | sodium channel | *Phyllobates terribilis*

Poison-dart *Phyllobates terribilis* frogs (also known as golden poison frogs) sequester various diet-derived alkaloid toxins in their granular skin glands as a chemical defense mechanism against predators (1). Among these alkaloids, batrachotoxin (BTX) is the most toxic molecule in poison darts made by Central American indigenous people. BTX has a rigid steroidal core structure with a tertiary amine (Fig. 1*A*; 538 Da; $pK_a \sim 7.5$). BTX targets voltage-gated Na^+ channels, which are essential for the generation and propagation of action potentials in excitable membranes (2). The actions of BTX on Na^+ channels are far reaching. First, BTX shifts the activation threshold by −30 to −50 mV so that Na^+ channels open readily at the resting membrane potential. Second, BTX eliminates both fast and slow inactivation of Na^+ channels, resulting in Na^+ channel opening that lasts for minutes. Third, BTX reduces single channel conductance as well as alters ion selectivity of the Na^+ channel.

The levels of BTX vary greatly among *Phyllobates* frogs, ranging from undetectable (*Phyllobates lugubris*) to up to 1.9 mg per adult frog (*P. terribilis*) (3). The average *P. terribilis* frog contains ∼1 mg of BTX, enough to kill more than 20,000 mice (minimal lethal dose ∼0.04 μg) (4). To understand how these frogs avoid BTX self-intoxication, Daly et al. (3) first reported that *P. terribilis* muscle Na^+ channels were insensitive to BTX. Their conclusion was based on the observation that BTX at 5 μM failed to depolarize membrane potentials of *P. terribilis* muscle cells. Breeding experiments indicated that BTX autoresistance in the *P. terribilis* frog was heritable. The genetic basis for this BTX autoresistance, however, remains unresolved to date. The α-subunit of the voltage-gated Na^+ channel consists of four repeated domains (D1–D4) each with six transmembrane segments (S1–S6) (5) (Fig. 1*B*). The BTX receptor within Na^+ channel isoforms has been mapped within the inner cavity along the S6 segments. All four S6 segments are involved in BTX binding interactions (6–8) (Fig. 1*B*, arrows).

Based on targeted sequencing data in 24 dendrobatids and six other frog species at D1/S6 and D4/S6 regions, Tarvin et al. (9) identified five AA substitutions (Fig. 1*C*) between frog *P. terribilis* muscle Na^+ channel and rat *Rattus norvegicus* at D1/S6 (S429A, I433V, and A445D as in rNav1.4) and D4/S6 (V1583I and N1584T). Ancestral state reconstruction showed that three substitutions (I433V, A445D, and V1583I) evolved multiple times independently in various poison frog clades. The other two substitutions (S429A and N1584T) evolved once in the most toxic species, *P. terribilis*. Their unprecedented sequencing data therefore provide us a genetic clue for autoresistance in poison frogs with alkaloid toxins, including BTX, histrionicotoxins (HTX), and pumiliotoxins (PTX) (9). Within these five AAs, we noticed that two of them, positions I433V at D1/S6 and N1584T at D4/S6, were previously proposed as parts of the BTX receptor. These earlier receptor-mapping studies were mostly based on lysine (K) substitutions (e.g., I433K and N1584K) (7, 10). Interestingly, according to their docking models, Tarvin et al. (9) found that autoresistance to BTX in *P. terribilis* was likely conferred by S429A and V1583I substitutions. In this study, we address whether these five naturally occurring AA substitutions are essential for BTX autoresistance in the *P. terribilis* frog both individually and in combination.

Results

BTX-Sensitive rNav1.4 Na^+ Channel. We used wild-type rat Nav1.4 Na^+ channels as a model system for this study, since the BTX

Significance

***Phyllobates terribilis* frog is listed as an endangered species, endemic to the Pacific coast of Colombia. Through diets, these golden poison frogs sequester lethal amounts of batrachotoxin in their skin for self-defense. Batrachotoxin activates voltage-gated Na^+ channels and keeps them open persistently with deadly consequences. This study addresses how golden poison frogs may avoid poisoning themselves via a naturally occurring substitution at the batrachotoxin receptor within their muscle Na^+ channel. An equivalent asparagine-to-threonine substitution not only preserved the functional integrity of rat muscle Na^+ channels but also rendered them exceptionally resistant to batrachotoxin. Such a switch could evolve via a single nucleotide mutation.**

Author contributions: S.-Y.W. and G.K.W. designed research, performed research, and wrote the paper.

The authors declare no conflict of interest.

This article is a PNAS Direct Submission.

[1]To whom correspondence should be addressed. Email: sywang@albany.edu.

PHARMACOLOGY

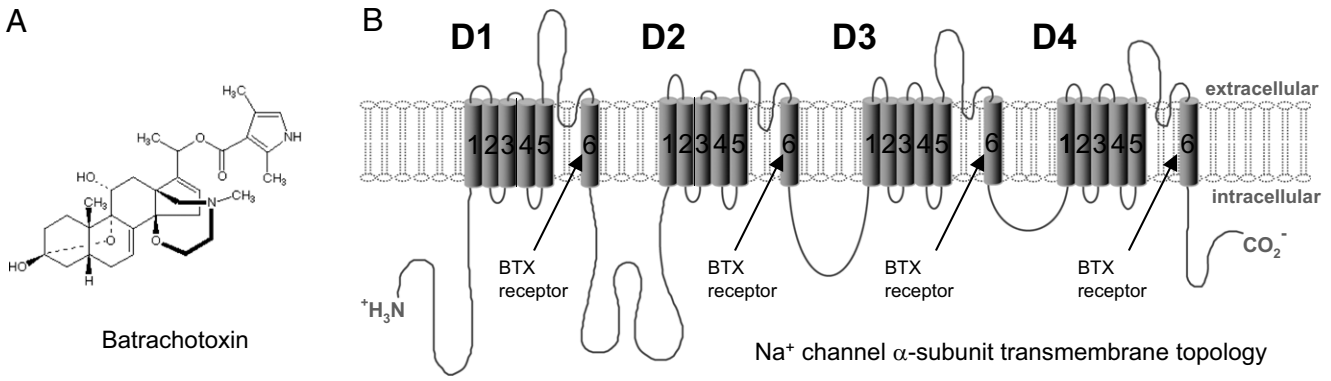

C

Nav1.4 (rat)	D1S6 segment	YMIFF VVIIF LG**S**FY L**I**NLI LAVVA MAY**A**
Nav1.4 (*P. terribilis*)	D1S6 segment	YMIFF VVIIF LG**A**FY L**V**NLI LAVVA MAY**D**
Nav1.4 (rat)	D4S6 segment	GICFF CSYII ISFLI V**VN**MY IAIIL ENFN
Nav1.4 (*P. terribilis*)	D4S6 segment	GICFF CSYII ISFLI V**IT**MY IAIIL ENFN

Fig. 1. (*A*) Chemical structure of batrachotoxin. (*B*) Transmembrane topology of the voltage-gated Na^+ channel α-subunit. The cylinders embedded in the lipid bilayer represent the transmembrane α-helical segments (S1–S6) of domains D1–D4. Arrows indicate the BTX receptor at the inner cavity. (*C*) AA sequences within D1/S6 and D4/S6 of the muscle Na^+ channel (Nav1.4) from *R. norvegicus* and *P. terribilis*. Five AA substitutions in D1/S6 and D4/S6 of *P. terribilis* muscle Na^+ channel (9) are highlighted in green.

receptor in this muscle Na^+ channel isoform has been mapped (6). As reported previously for *P. terribilis* muscle cells (3), we applied BTX at a saturating concentration of 5 μM. Under our experimental conditions, wild-type rNav1.4 Na^+ channels were activated around −50 mV and rNav1.4 Na^+ currents decayed rapidly due to fast inactivation (11). Fig. 2 shows the phenotypes regarding BTX modifications of Nav1.4 Na^+ channels. First, most of transient fast-inactivating Na^+ currents became noninactivating after 1,500 repetitive pulses of +50 mV for 20 ms at 2 Hz (Fig. 2*A*). At pulse 1 trace, some of the transient Na^+ currents were already modified by BTX, which occurred during the 10- to 15-min wait time for whole-cell dialysis. Second, once modified, these noninactivating currents (Fig. 2*B*) were long lasting throughout the 500-ms pulse duration at various voltages. The activation threshold was also leftward shifted by BTX so that inward Na^+ current first appeared at −80 mV (Fig. 2*B*).

Because BTX eliminates both fast and slow inactivation of Na^+ channels (2), BTX-modified Na^+ currents can also be conveniently recorded using a 1-s ramp stimulus from −140 mV to +50 mV as shown in Fig. 2*C*. The activation threshold of these

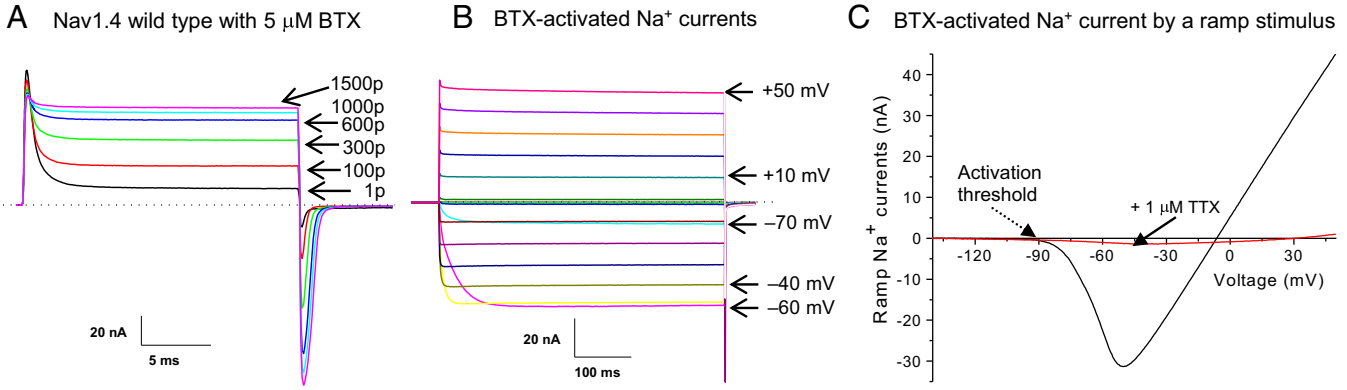

Fig. 2. Nav1.4 wild-type Na^+ channels modified by 5 μM BTX. (*A*) Superimposed traces of Nav1.4 Na^+ currents at 5 μM BTX were recorded during repetitive pulses (+50 mV for 20 ms at 2 Hz). Current traces correspond to pulses of 1, 100, 300, 600, 1,000, and 1,500. Transient Na^+ currents became progressively noninactivating and persistent even near the end of the 20-ms pulse. Most of transient Na^+ currents were converted to noninactivating after 1,500 pulses (maintained vs. peak, 92.0 ± 3.1%; $n = 9$). The dashed line indicates the current baseline. (*B*) BTX eliminated both fast and slow inactivation of Nav1.4 Na^+ channels. Currents were generated at voltages from −120 mV to +50 mV for 500 ms in 10-mV increments. Most Na^+ currents were noninactivating during the pulse. The labels near current traces correspond to the voltages applied. (*C*) After 1,500 repetitive pulses, a 1-s ramp stimulus from −140 mV to +50 mV was used to generate BTX-modified Na^+ currents. The ramp Na^+ currents were then plotted against voltage. The activation threshold, defined as inward BTX-modified Na^+ currents first appeared from the baseline (dashed arrow) during a ramp stimulus, was recorded around −90 mV (−90.8 ± 2.0 mV; $n = 9$). Inward currents reached peak amplitude around −50 mV and then decreased; outward currents appeared around −10 mV and increased linearly with a maximal value of 45 nA (34.2 ± 8.3 nA; $n = 9$) at +50 mV. TTX at 1 μM blocked most of BTX-modified Na^+ currents except for a small background current (trace in red; solid arrow). Current traces in different panels were recorded from different cells. Holding potential was set at −140 mV. p, pulse(s).

BTX-modified Na^+ channels was measured around −90 mV, where inward Na^+ currents first appeared from the baseline during a ramp stimulus (Fig. 2*C*, dashed arrow). This activation threshold was much lower than that of the wild-type Na^+ channels (approximately −50 mV). Inward ramp Na^+ currents reached their maximum around −50 mV and then reversed their direction, whereas outward Na^+ currents first appeared near −10 mV and increased linearly until the ramp stimulus ended at +50 mV. Tetrodotoxin (TTX) at 1 μM blocked most of ramp BTX-modified Na^+ currents (Fig. 2*C*, red trace), confirming that rNav1.4 Na^+ channels were TTX sensitive.

In the remaining section, we define BTX-sensitive Na^+ channels with three criteria. First, the ratio of the noninactivating vs. the peak Na^+ current is ≥75% after 1,500 repetitive pulses. Second, a 1-s ramp stimulus will generate robust BTX-modified ramp Na^+ currents. Third, the activation threshold of BTX-modified ramp Na^+ currents occurs at ≤−80 mV.

A Complete BTX-Resistant 5AA-Mutant Na^+ Channel. We created an rNav1.4 mutant with five AA substitutions on D1/S6 and D4/S6 (Fig. 1*C*) and tested whether such a 5AA-rNav1.4 mutant channel is sensitive to BTX. Fig. 3*A* shows that this 5AA mutant (Nav1.4-S429A/I433V/A445D/V1583I/N1584T) was completely resistant to BTX after 1, 100, 500, 1,000, 1,500, and up to 2,000 repetitive pulses (+50 mV for 20 ms at 2 Hz). The residual maintained current after 1,500 pulses was relatively small compared with the peak current amplitude (1.1 ± 0.3%, n = 16). Nonetheless, this residual current could in part come from the background current at +50 mV as shown in Fig. 2*C* in the presence of 1 μM TTX. There appeared a gradual reduction of peak Na^+ currents, likely due to cumulative slow inactivation during repetitive pulses. Our result thus revealed clearly that these five naturally occurring substitutions found in *P. terribilis* frogs could be involved in BTX autoresistance. Fig. 3*B* shows the conductance vs. voltage relationship of the 5AA-rNav1.4 mutant channel. Data were calculated from peak mutant Na^+ currents generated at various voltages. Activation threshold of 5AA mutant Na^+ channels appeared around −40 mV. The 50% conductance ($E_{0.5}$) occurred at −7.4 ± 1.2 mV with a slope factor (k_a) of 15.2 ± 1.0 mV (n = 16) (Fig. 3*B*). These fitted gating parameters are significantly different (P < 0.05) from those of the wild-type counterparts ($E_{0.5}$ = −32.7 ± 1.4 mV and k_a = 10.0 ± 1.2 mV; n = 5) (11).

Fig. 3*C* shows the steady-state fast inactivation (h_∞ curve) of five-AA mutant channel at various conditioning pulses for 100 ms. Most mutant Na^+ currents were fast inactivated at voltage greater than or equal to −50 mV; there were no noninactivating Na^+ currents present above this voltage. The 50% steady-state inactivation ($h_{0.5}$) corresponded to −83.9 ± 0.2 mV (with a slope factor k_h of 6.2 ± 0.1 mV, n = 16); at this voltage, 50% of Na^+ channels were fast inactivated (Fig. 3*C*). These fitted gating parameters are also significantly different (P < 0.01) from those found in the wild-type counterpart ($h_{0.5}$ = −74.5 ± 0.5 mV and k_h = 5.5 ± 0.1 mV; n = 5) (11). This phenomenon about gating alternations in 5AA-mutant channels is not unique, since AA substitutions at S6 regions tend to change Na^+ channel gating parameters rather significantly (12–14). With 72% AA sequence identity between rat and amphibian muscle Na^+ channels, whether such alternations in rNav1.4 channels are relevant to the muscle Na^+ channel function in *P. terribilis* frogs is uncertain. After 1,500 repetitive pulses at 5 μM BTX, we did not observe any BTX-modified ramp Na^+ currents from this 5AA mutant with a 1-s ramp stimulus. The absence of a noticeable ramp Na^+ current is understandable because BTX-resistant mutant Na^+ channels are all fast inactivated before the slow ramp depolarization reaches the activation threshold (Fig. 3 *B* vs. *C*).

In the remaining section, we define the complete BTX-resistant Na^+ channel with the following criteria. First, little or no maintained Na^+ currents appear after 1,500 repetitive pulses at 5 μM BTX. Second, the fast decaying phase of the transient Na^+ current is little changed by BTX. Third, little or no BTX-modified ramp Na^+ currents emerge during a 1-s ramp stimulus.

BTX-Sensitive and BTX-Resistant Mutants with a Single AA Substitution. Are all these five naturally occurring substitutions critical for BTX autoresistance in poison-dart *P. terribilis* frogs? To address this question, we screened five individual mutants each with a single AA substitution. Our data showed that, except N1584T, all individual mutants were sensitive to BTX (Figs. 4 and 5) as determined by our BTX-sensitive criteria. First, single mutants (S429A, I433V, A445D, and V1583I) were readily modified by 5 μM BTX during repetitive pulses up to 1,500 pulses (Figs. 4 *A* and *C*

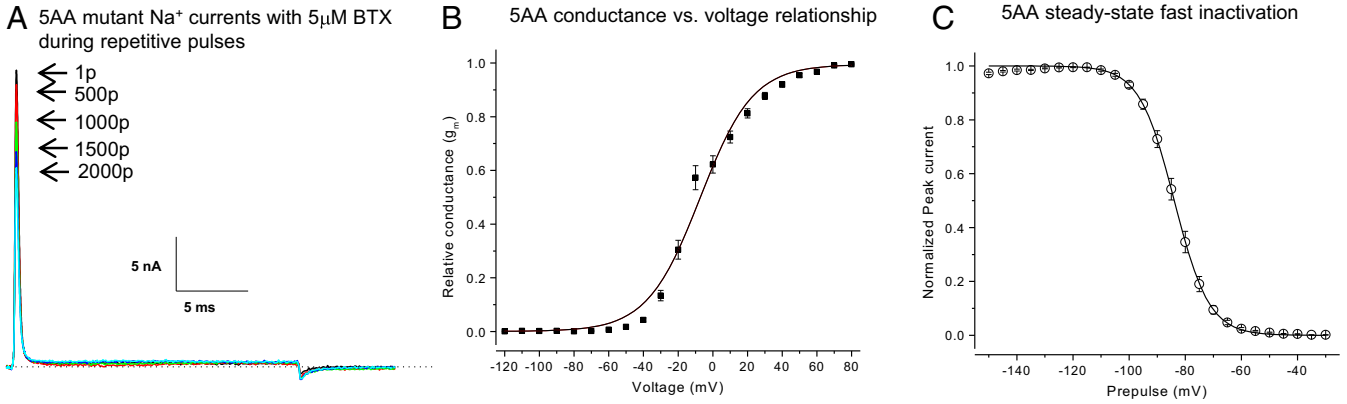

Fig. 3. A complete BTX-resistant phenotype in 5AA-rNav1.4 mutant channels. (*A*) Superimposed traces of 5AA mutant Na^+ currents were recorded during repetitive pulses (+50 mV for 20 ms at 2 Hz). The pipette solution contained 5 μM BTX. The arrows correspond to the current traces after 1, 500, 1,000, 1,500 and 2,000 pulses. The residual maintained current after 1,500 pulses was small (1.1 ± 0.3% of the peak amplitude, n = 16). (*B*) For the current–voltage relationship, peak Na^+ currents were recorded at various voltages in 10-mV increments from −120 to +80 mV for 10 ms. Peak Na^+ currents were measured, converted to conductance, normalized with respect to conductance at +80 mV, and plotted against voltage. Conductance was determined by the equation $g_m = I_{Na}/(E_m - E_{Na})$, where I_{Na} is the peak current amplitude; E_m is the voltage applied, and E_{Na} is the estimated reversal potential (11). The plot was fitted with a Boltzmann function, which gave a midpoint voltage ($V_{0.5}$) and a slope factor (k_a) of −7.4 ± 1.2 mV and 15.2 ± 1.0 mV, respectively (n = 16). (*C*) The steady-state inactivation (h_∞) was measured by a conventional 2-pulse protocol (11). Currents were evoked by 5-ms test pulses to +50 mV after 100-ms conditioning pulses ranging from −150 to −30 mV in 5-mV increments. Peak currents at the test pulse were measured, normalized with respect to the maximal peak current, and plotted against the conditioning voltage. The plot was fitted with a Boltzmann function; the fitted midpoint ($h_{0.5}$) and slope factor (k_h) were −83.9 ± 0.2 mV and 6.2 ± 0.1 mV (n = 16), respectively. p, pulse(s).

and 5 *A* and *C*) in a manner resembling that of wild-type rNav1.4 Na^+ channels (Fig. 2*A*). The maintained currents reached ≥75% of the peak amplitude after 1,500 pulses for all four BTX-sensitive mutant channels. Second, BTX shifted the activation threshold of these mutant channels leftward to around −90 to −100 mV under a 1-s ramp stimulus (Figs. 4 *B* and *D* and 5 *B* and *D*). Third, the presence of noninactivating persistent currents and the robust ramp-generated BTX-modified Na^+ currents (Figs. 4 and 5) showed clearly that BTX eliminated both fast and slow inactivation of these mutants.

In contrast, the N1584T mutant exhibited a unique BTX-resistant phenotype. Like all other mutants, this N1584T mutant preserved its functional integrity of fast inactivation as transient mutant Na^+ currents declined rapidly to the baseline after it reached its peak (Fig. 6*A*). Curiously, we observed that during repetitive pulses, a small slow-decaying component of Na^+ currents became visible at 5 μM BTX. However, the magnitude of this slowing effect was rather limited and transient mutant Na^+ currents still decayed to the baseline within a few milliseconds (Fig. 6*A*, dashed arrow). After 1,500 repetitive pulses, we also did not detect ramp Na^+ currents generated by N1584T mutant channels using a 1-s ramp stimulus. By our definition, the N1584T mutant did not qualify as a complete BTX-resistant mutant. The exact nature of this small BTX residual effect on the rNav1.4-N1584T mutant channel (Fig. 6*A*, dashed arrow) is unclear but the magnitude appears too small to have any physiological consequences. This residual effect was not recorded in the five-AA mutant as shown in Fig. 3*A*, suggesting that four other substitutions (S429A, I433V, A445D, and V1583I) may help remove such effect found in the N1584T mutant. We thus categorize this N1584T mutant as an exceptionally BTX-resistant Na^+ channel that fails to generate noninactivating late Na^+ currents or ramp Na^+ currents at 5 μM BTX. Overall, the data on five single mutants led us to conclude that only one residue, N1584T, plays a critical and dominant role pertaining to BTX autoresistance in *P. terribilis* frogs.

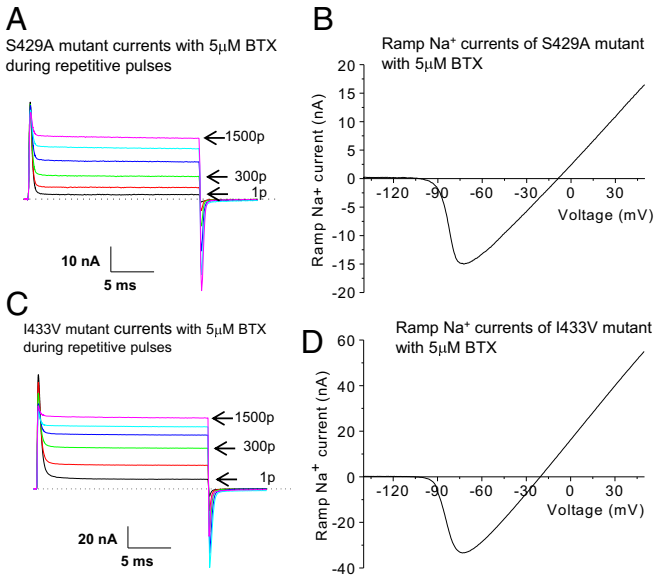

Fig. 4. A BTX-sensitive phenotype in mutants of S429A and I433V. (*A*) Superimposed traces of S429A-rNav1.4 Na^+ currents were recorded during repetitive pulses (+50 mV for 20 ms at 2 Hz). At 5 μM BTX, most of transient Na^+ currents were converted to noninactivating and maintained at the end of the pulse. Repetitive pulses gradually reduced the peak amplitude. Current traces correspond to 1, 100, 300, 600, 1,000, and 1,500 pulses applied. The noninactivating current after 1,500 repetitive pulses reached 90% of the peak current amplitude (85.5 ± 3.2%; $n = 8$). (*B*) After 1,500 repetitive pulses, S429A-rNav1.4 Na^+ currents were recorded by a 1-s ramp stimulus from −140 mV to +50 mV and plotted against voltage as describe in Fig. 2*C*. The BTX-modified Na^+ currents were activated near −100 mV (−100.6 ± 1.6 mV; $n = 8$) and reached its maximal outward current of 17 nA at +50 mV (24.6 ± 3.2 nA; $n = 8$). (*C*) Superimposed traces of I433V-rNav1.4 Na^+ currents were shown using the same pulse protocol as in *A*. Most transient Na^+ currents were converted to noninactivating (86.8 ± 3.1%; $n = 8$). Current traces correspond to 1, 100, 300, 600, 1,000, and 1,500 pulses applied. (*D*) Ramp I433V-rNav1.4 Na^+ currents were plotted against voltage as described in Fig. 2*C*. The BTX-modified currents were activated near −100 mV (−92.6 ± 3.4 mV; $n = 8$) and reached the maximal value of 55 nA (38.3 ± 8.5 nA; $n = 8$) at +50 mV. The pipette solution contained 5 μM BTX. p, pulse(s).

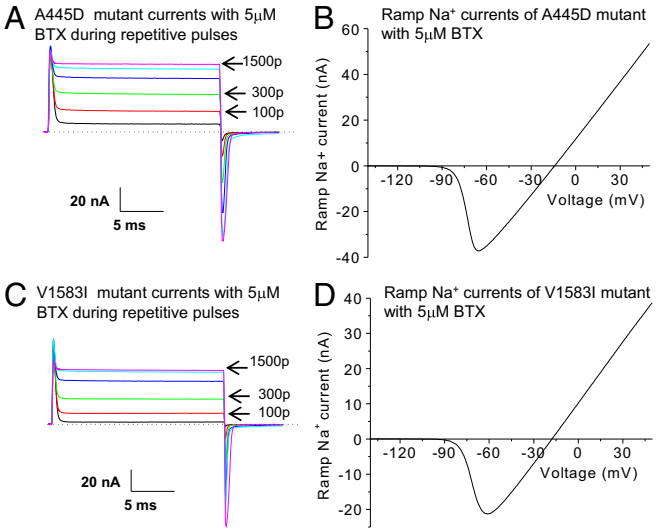

Fig. 5. A BTX-sensitive phenotype in mutants of A445D and V1583I. (*A*) Superimposed traces of A445D-rNav1.4 Na^+ currents were recorded during repetitive pulses as described (+50 mV for 20 ms at 2 Hz). Most of transient Na^+ currents were converted to noninactivating after 1,500 pulses (84.6 ± 2.0%; $n = 9$). Repetitive pulses also gradually reduced the peak amplitude. Current traces correspond to 1, 100, 300, 600, 1,000, and 1,500 pulses applied. (*B*) Ramp A445D-rNav1.4 Na^+ currents were recorded by a 1-s ramp stimulus after 1,500 repetitive pulses. The ramp Na^+ currents were then plotted against voltage. The BTX-modified Na^+ currents were activated near −90 mV (−95.6 ± 3.0 mV; $n = 9$) and reached the maximal value of 55 nA at +50 mV (34.6 ± 6.2 nA; $n = 9$). (*C*) Superimposed traces of V1583I-rNav1.4 Na^+ currents were shown using the same pulse protocol (+50 mV for 20 ms at 2 Hz). Most transient Na^+ currents were converted to noninactivating after 1,500 pulse (86.1 ± 1.5%; $n = 9$). Current traces correspond to 1, 100, 300, 600, 1,000, and 1,500 pulses applied. (*D*) Ramp V1583I-rNav1.4 Na^+ currents were recorded by a 1-s ramp stimulus after 1,500 repetitive pulses and plotted against voltage as described in Fig. 2*C*. The BTX-modified Na^+ currents were activated near −90 mV (−92.0 ± 1.7 mV; $n = 9$), whereas the outward currents reached the maximal value of 40 nA (34.1 ± 5.7 nA; $n = 9$). The pipette solution contained 5 μM BTX. p, pulses.

Screening of Additional Combination Mutants with More than One AA Substitution. To substantiate the dominant role of an N1584T substitution in BTX action, we created two additional combination mutants. Both mutants with an inclusion of N1484T (Nav1.4-A445D/V1583I/N1584T and Nav1.4-S429A/I433V/V1583I/N1584T) exhibited a BTX-resistant phenotype as described in the five-AA mutant (Fig. 3*A*) and qualified as complete BTX-resistant mutants. Fig. 6*B* shows the current recordings of Nav1.4-A445D/V1583I/N1584T mutant channels during repetitive pulses. In the presence of 5 μM BTX, this mutant remained functional with fast inactivation intact; all transient Na^+ currents decayed rapidly with little or no noninactivating late currents during repetitive pulses. There was no evidence that a residual BTX effect existed in the Nav1.4-A445D/V1583I/N1584T mutant compared with that found in the N1584T counterpart (Fig. 6 *A* vs. *B*). With a 1-s ramp stimulus, we did not detect any ramp Na^+ currents generated by this combination mutant channel.

We next tested whether a combination of two or more AA substitutions without N1584T may together contribute to BTX

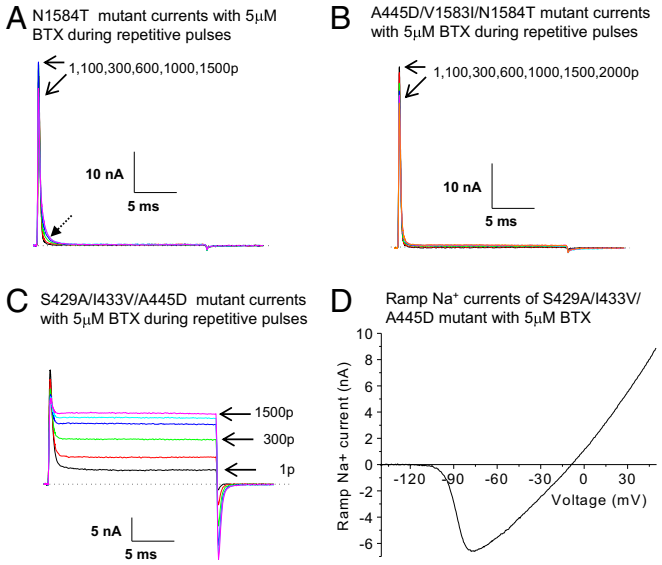

Fig. 6. BTX-resistant and BTX-sensitive phenotypes in single and combination mutants. (*A*) Superimposed traces of N1584T-rNav1.4 Na^+ currents were recorded during repetitive pulses (+50 mV for 20 ms at 2 Hz). The arrows indicate the current traces after 1 pulse and 1,500 pulses, respectively. Little or no noninactivating persistent currents were evident after 1,500 pulses (1.8 ± 0.6%; $n = 8$). A small residual slowing effect on the decaying phase of the transient Na^+ currents was detected in all recorded cells (dashed arrow). This slow decaying component could be best fitted by an exponential function with a τ-value of 0.55 ± 0.03 ms ($n = 8$; at 1,500 pulses), whereas the fast component had a τ-value of 0.25 ± 0.02 ms ($n = 8$). (*B*) Superimposed traces of A445D/V1583I/N1584T-rNav1.4 Na^+ currents were recorded during repetitive pulses (+50 mV for 20 ms at 2 Hz). A complete BTX-resistant phenotype of this combination mutant was evident, which resembled that of the 5AA mutant shown in Fig. 3*A*. The arrows indicate the current traces after 1 pulse and 2,000 pulses, respectively. The maintained current was about 1% of the peak amplitude after 1,500 pulses (0.8 ± 0.4%; $n = 8$). (*C*) Superimposed traces of S429A/I433V/A445D-rNav1.4 Na^+ currents were recorded during repetitive pulses (+50 mV for 20 ms at 2 Hz). Most transient Na^+ currents were converted to noninactivating after 1,500 pulses (85% of the peak amplitude; 86.0 ± 2.8%; $n = 5$). This BTX-sensitive phenotype of S429A/I433V/A445D-rNav1.4 Na^+ currents resembled that of wild-type rNav1.4 counterparts shown in Fig. 2*A*. Current traces correspond to 1, 100, 300, 600, 1,000, and 1,500 pulses applied. (*D*) After 1,500 pulses, ramp Na^+ currents through the S429A/I433V/A445D-rNav1.4 mutant channels were recorded using a 1-s ramp stimulus from −140 mV to +50 mV and plotted against voltage. Inward BTX-modified Na^+ currents were activated near −105 mV (−104.6 ± 2.0 mV; $n = 5$) and reached the maximal value of 9 nA (13.9 ± 2.2 nA; $n = 5$). The pipette solution contained 5 μM BTX. p, pulse(s).

autoresistance. Accordingly, we screened four additional combination mutants (Nav1.4-S429A/I433V, Nav1.4-A445D/V1583I, Nav1.4-S429A/I433V/445D, and Nav1.4-S429A/I433V/A445D/V1583I) for their BTX sensitivity. We found that these combination mutants all qualified as BTX-sensitive mutant channels. Fig. 6*C* shows the current recordings of the Nav1.4-S429A/I433V/A445D mutant channel, which includes all three AA substitutions at D1/S6. After 1,500 repetitive pulses, most of the transient Na^+ currents became noninactivating at 5 μM BTX. With a 1-s ramp stimulus, ramp Na^+ currents were conspicuous and the activation threshold for this mutant channel appeared around −105 mV (Fig. 6*D*).

Discussion

We have demonstrated that rNav1.4 combination mutant channels with an N1584T substitution (e.g., Figs. 3*A* and 6*B*) all confer complete BTX autoresistance first reported in *P. terribilis* muscle cells (3). The other four naturally occurring substitutions play a minimal role in BTX autoresistance. Collectively, after 1,500 pulses the ratios of the maintained vs. the peak current of all BTX-sensitive mutants are not significantly different from that of the wild-type channels at 5 μM BTX ($P > 0.05$), whereas those of BTX-resistant mutants are ($P < 0.0001$) (Figs. 2*A*–6*C*). Furthermore, we have established that a single N1584T substitution abolishes all BTX actions on the rNav1.4 Na^+ channel in a nearly complete manner (Fig. 6*A*). This single substitution alone could explain why *P. terribilis* frogs survive in the wild even though they contain ∼1.1 mg of BTX per adult. Such a large BTX quantity would require robust BTX autoresistance in these golden poison frogs. This N1584T substitution could occur naturally via a single nucleotide replacement (AAC→ACC) (9).

Unexpectedly, poison-dart *Phyllobates aurotaenia* frogs do not possess this N1584T substitution (9) despite the fact that these frogs contain ∼50 μg BTX per adult (3, 4). Although none of the five AA substitutions evolved deep in the dendrobatid phylogeny, Tarvin et al. (9) hypothesized that the V1583I substitution facilitates the evolution of extreme toxicity in *P. terribilis*. This hypothesis is based on two observations that (*i*) only this V1583I substitution occurs simultaneously in *P. terribilis* and *P. aurotaenia* and (*ii*) protein-docking analyses indicate a decrease in BTX binding affinity by the V1583I substitution. Since our data showed that Nav1.4-V1583I mutant channels remained BTX sensitive (Fig. 5 *C* and *D*), the evolutionary role of this substitution remains unresolved. It is feasible that V1583I alone or with additional S6 substitutions (e.g., Figs. 3*A* and 6*B*) might play a part to eliminate the small residual BTX effect found in the N1584T mutant (Fig. 6*A*, dashed arrow). Alternatively, this V1583I substitution may be important for autoresistance to HTXs and PTXs found in various *Phyllobates* poison frogs (1, 9). Importantly, the cloning of *P. aurotaenia* muscle Nav1.4 isoform and its expression in *Xenopus* oocytes revealed that an intermediate BTX-resistant phenotype (15) could exist in the *Phyllobates* clade as an evolutionary option (9). This BTX-resistant phenotype (∼20–50% ratio of maintained to peak currents at +80 mV with 10 μM BTX) may allow *P. aurotaenia* frog to survive since its skin contains less BTX.

How does an N1584T substitution give rise to an exceptionally BTX-resistant phenotype? We have shown previously that the N1584 residue in the rNav1.4 Na^+ channel is critical for BTX action on voltage-gated Na^+ channels (10). With a lysine replacement (N1584K), rNav1.4 Na^+ channels became completely resistant to BTX, comparable to that found in N1584T combination mutants. With an alanine (N1584A) or an aspartic acid (N1584D) replacement, intermediate BTX-resistant phenotypes were recorded. For example, BTX partially inhibited fast and slow inactivation of N1584D mutant channels as their BTX-modified Na^+ currents decayed extensively during a prolonged depolarization to +50 mV, a phenotype very different from that of BTX-modified wild-type Na^+ channels (Fig. 2*B*). As for the N1584A mutant, its BTX-modified phenotype included mainly a slowing effect on the decaying phase of transient Na^+ currents during repetitive pulses. The slowing effect manifested in N1584A mutant channels by BTX (10) was somewhat more severe than that found in the N1584T mutant (Fig. 6*A*, dashed arrow). These observations illustrate the important role of the N1584 side-chain moiety in BTX actions on Na^+ channels. It is noteworthy that more than 20% of the peak currents carried by N1584K mutant channels were noninactivating during a +50-mV test pulse, indicating that this mutant channel is inherently inactivation deficient (10). The presence of small noninactivating late Na^+ currents (i.e., gain of function) is known to cause various muscle channelopathies (16). With regard to the N1584A mutant, its expression in HEK293 cells was generally poor (<1 nA) (10). Thus, instead of N1584K or N1584A substitution, *P. terribilis* poison frogs become BTX resistant via an equivalent N1584T substitution, which keeps Na^+ channel fast inactivation nearly intact even in the presence of 5 μM BTX. These genotype–phenotype associations in BTX resistance along with inactivation deficiency and reduced expression among N1584K/A/D/T mutants together support the

notion that functional constraint shapes the evolution of the *P. terribilis* Nav1.4 inner cavity (9).

Recently, two reports from the Du Bois' laboratory described the organic syntheses of various BTX analogs and enantiomeric BTX toxins (17, 18). These authors discovered a family of BTX analogs and nonnatural (+)-BTX toxins as reversible channel blockers. In particular, among all S6 substitutions, they found that N1584K had the most destabilizing effect on the binding of BTX analogs and (+)-BTX enantiomer. Based on their site-directed mutagenesis results, they provided a 3D rNav1.4 homology model, which depicted the N1584 residue as a part of the BTX receptor within Na^+ channel inner cavity. Cautions should be taken, since their homology structure is derived from bacterial Nav crystallographic data (9, 11, 19). Nonetheless, our results strongly support the conclusion that BTX autoresistance in *P. terribilis* muscle Na^+ channels is primarily due to an equivalent rNav1.4-N1584T substitution, which eliminates nearly all BTX actions. This N1584 residue probably functions as an integral part of the BTX receptor in the rNav1.4 Na^+ channel. Finally, we envision that *P. terribilis* muscle Na^+ channels once available will display a complete BTX-resistant phenotype as found in five-AA mutant channels (Fig. 3*A*). Whether a reverse mutant (T1584N equivalent in such channel) remains partially BTX resistant as predicted by stepwise increases of toxin autoresistance in poison frogs during evolution (9) merits additional studies. Such stepwise increase of BTX autoresistance, if true, could derive from substitutions in D2S6, D3S6 (15, 20), or elsewhere (11).

Materials and Methods

Site-Directed Mutagenesis. We used the QuikChange XL site-directed mutagenesis kit (Stratagene) to create all rNav1.4 mutants within the pcDNA1/Amp vector (11). Mutants with single AA substitutions were created first, which included: rNav1.4-S429A, I433V, A445D, V1583I, and N1584T. Mutants with a combination of these five amino acids were chosen in two groups. One group, which included the N1584T substitution, contained the following mutants: 445D/1583I/1584T, S429A/I433V/V1583I/N1584T, and S429A/I433V/A445D/V1583I/N1584T with all five AA substitutions (i.e., 5AA mutant). The other group, all without the N1584T substitution, included the following mutants: S429A/I433V, S429A/I433V/A445D, and S429A/I433V/A445D/V1583I.

Cell Culture and Transient Transfection of HEK Cells. HEK293t cells were maintained in Ti25 flasks at 37 °C in a 5% CO_2 incubator in DMEM (Life Technologies) containing 10% FBS (HyClone) and 1% penicillin and streptomycin solution (Sigma) (7). HEK293t cells expressing rNav1.4 wild-type and mutant Na^+ channels along with β1-subunit and CD8 surface antigen were prepared by transient transfection via a calcium phosphate precipitation method and used within 2–4 d after transfection (14).

Electrophysiology, Data Acquisition, and Statistics. Transfected HEK293t cells were replated in 30-mm dishes, which were used as recording chambers. Cells that expressed the CD8 antigen (identifiable by antibody-coated beads) (Dynabeads M-450 CD8, Life Technologies) were selected for patch-clamp experiments. Individual cells were superfused with an extracellular solution containing (in millimoles) 65 NaCl, 85 choline-Cl, 2 $CaCl_2$, and 10 Hepes (titrated with tetramethylammonium-OH to pH 7.4). The pipette (intracellular) solution consisted of (in millimoles) 100 NaF, 30 NaCl, 10 EGTA, and 10 Hepes (titrated with cesium-OH to pH 7.2). BTX was a gift from John Daly (NIH, Bethesda) and was dissolved in DMSO at 0.5 mM. BTX was added into the pipette solution to a final concentration of 5 μM. DMSO (up to 1%) in the bath or in the pipette solution had little effect on Na^+ currents. TTX was purchased from Calbiochem (EMD Millipore) and was dissolved in distilled water at 1 mM. A final concentration of 1 μM TTX was made by dilution with the extracellular solution.

The whole-cell configuration of a patch-clamp technique (21) was used to record Na^+ currents in HEK293t cells at room temperature (22 ± 2 °C). Electrode resistance ranged from 0.4 to 0.6 MΩ. Command voltages were elicited with pCLAMP9 software and delivered by Axopatch 200B (Molecular Devices, Inc.). Cells were held at −140 mV and dialyzed for 10–15 min. During this time, Na^+ currents were monitored infrequently by test pulses (+50 mV/10 ms) at a 30-s interval. The capacitance and leak currents were cancelled with the patch-clamp device and by P/−4 subtraction. Access resistance was about 1 MΩ under the whole-cell configuration; series resistance compensation of ≥95% resulted in voltage errors of ≤3 mV at +50 mV. For both step and ramp stimuli, the voltage error was negligible around the activation threshold and comparatively small during channel activation, where the inward Na^+ current amplitudes were modest. Pipettes with larger access resistance (>1.5 MΩ) were undesirable since it would limit BTX diffusion into the intracellular fluid. Repetitive pulses of +50 mV/20 ms were applied at 2 Hz to facilitate BTX binding with the open Na^+ channels and the resulting outward Na^+ currents were recorded (7). In rare cases, repetitive pulses of +30 mV/20 ms were used when the current amplitude at +50 mV reached the limit of the amplifier. Such recordings allowed us to avoid the complication of series resistance artifacts and also to circumvent inward Na^+ ion loading (22). Extracellular solutions were delivered via narrow-bored capillary tubes positioned within 300 μm from the cell. Curve fitting was performed using the program Microcal Origin. An unpaired Student's *t* test was used to evaluate estimated parameters (mean ± SEM or fitted value ± SE of the fit); *P* values of <0.05 were considered statistically significant.

ACKNOWLEDGMENTS. We are indebted to the late Dr. John Daly for his generous gift of BTX and his kind encouragement. This study was undertaken in part by the volunteer work of G.K.W. and was made possible by completed grants from NIH, HL66076 (to S.-Y.W.) and GM94152 (to G.K.W.).

1. Daly JW (1995) The chemistry of poisons in amphibian skin. *Proc Natl Acad Sci USA* 92: 9–13.
2. Hille B (2001) Modification of gating in voltage-sensitive channels. *Ion Channels of Excitable Membranes* (Sinauer Associates, Sunderland, MA), 3rd Ed, pp 635–662.
3. Daly JW, Myers CW, Warnick JE, Albuquerque EX (1980) Levels of batrachotoxin and lack of sensitivity to its action in poison-dart frogs (*Phyllobates*). *Science* 208: 1383–1385.
4. Myers CW, Daly JW, Malkin B (1978) A dangerously toxic new frog (*Phyllobates*) used by Emberá Indians of western Colombia, with discussion of blowngun fabrication and dart poisoning. *Bull Am Mus Nat Hist* 161:307–366.
5. Catterall WA (2012) Voltage-gated sodium channels at 60: Structure, function and pathophysiology. *J Physiol* 590:2577–2589.
6. Wang S-Y, Wang GK (2003) Voltage-gated sodium channels as primary targets of diverse lipid-soluble neurotoxins. *Cell Signal* 15:151–159.
7. Wang S-Y, Wang GK (1998) Point mutations in segment I-S6 render voltage-gated Na^+ channels resistant to batrachotoxin. *Proc Natl Acad Sci USA* 95:2653–2658.
8. Linford NJ, Cantrell AR, Qu Y, Scheuer T, Catterall WA (1998) Interaction of batrachotoxin with the local anesthetic receptor site in transmembrane segment IVS6 of the voltage-gated sodium channel. *Proc Natl Acad Sci USA* 95:13947–13952.
9. Tarvin RD, Santos JC, O'Connell LA, Zakon HH, Cannatella DC (2016) Convergent substitutions in a sodium channel suggest multiple origins of toxin resistance in poison frogs. *Mol Biol Evol* 33:1068–1081.
10. Wang S-Y, Wang GK (1999) Batrachotoxin-resistant Na^+ channels derived from point mutations in transmembrane segment D4-S6. *Biophys J* 76:3141–3149.
11. Wang SY, Mitchell J, Tikhonov DB, Zhorov BS, Wang GK (2006) How batrachotoxin modifies the sodium channel permeation pathway: Computer modeling and site-directed mutagenesis. *Mol Pharmacol* 69:788–795.
12. Yarov-Yarovoy V, et al. (2001) Molecular determinants of voltage-dependent gating and binding of pore-blocking drugs in transmembrane segment IIIS6 of the $Na(^+)$ channel α subunit. *J Biol Chem* 276:20–27.
13. Yarov-Yarovoy V, et al. (2002) Role of amino acid residues in transmembrane segments IS6 and IIS6 of the Na^+ channel α subunit in voltage-dependent gating and drug block. *J Biol Chem* 277:35393–35401.
14. Wang S-Y, Bonner K, Russell C, Wang GK (2003) Tryptophan scanning of D1S6 and D4S6 C-termini in voltage-gated sodium channels. *Biophys J* 85:911–920.
15. Frezza L, et al. (2010) Is the skeletal muscle sodium channel of the batrachotoxin (BTX)-producing *Phyllobates aurotaenia* poison dart frog resistant to BTX? *Biophys J* 98(Suppl 1):113a.
16. Cannon SC (1996) Sodium channel defects in myotonia and periodic paralysis. *Annu Rev Neurosci* 19:141–164.
17. Logan MM, Toma T, Thomas-Tran R, Du Bois J (2016) Asymmetric synthesis of batrachotoxin: Enantiomeric toxins show functional divergence against NaV. *Science* 354:865–869.
18. Toma T, Logan MM, Menard F, Devlin AS, Du Bois J (2016) Inhibition of sodium ion channel function with truncated forms of batrachotoxin. *ACS Chem Neurosci* 7: 1463–1468.
19. Zhorov BS, Tikhonov DB (2016) Computational structural pharmacology and toxicology of voltage-gated sodium channels. *Curr Top Membr* 78:117–144.
20. Du Y, Garden DP, Wang L, Zhorov BS, Dong K (2011) Identification of new batrachotoxin-sensing residues in segment IIIS6 of the sodium channel. *J Biol Chem* 286:13151–13160.
21. Hamill OP, Marty A, Neher E, Sakmann B, Sigworth FJ (1981) Improved patch-clamp techniques for high-resolution current recording from cells and cell-free membrane patches. *Pflugers Arch* 391:85–100.
22. Cota G, Armstrong CM (1989) Sodium channel gating in clonal pituitary cells. The inactivation step is not voltage dependent. *J Gen Physiol* 94:213–232.